Biointerface Research in Applied Chemistry
Platinum Open Access Journal (ISSN: 2069-5837)

Article
Volume 11, Issue 1, 2021, 8043 - 8051
https://doi.org/10.33263/BRIAC111.80438051

Synthesis and *in vitro* Evaluation of Thermosensitive *PLA-g-P(HEM-co-NIPAAM)* Hydrogel Used for Delivery of VEGF

Baharak Divband [1,2], Mohammad Samiei [1,3], Soodabeh Davaran [4], Leila Roshangar [5], Shahriar Shahi [1,3,*], Marziyeh Aghazadeh [6,]**

1 Dental and Periodontal Research Center, Tabriz University of Medical Sciences, Tabriz. Iran; bdivband@gmail.com, divband@tabrizu.ac.ir (B.D.); samiei.moh@gmail.com (M.S.); sshahriar32@gmail.com (S.S.);
2 Inorganic Chemistry Department, Faculty of Chemistry, University of Tabriz, Iran;
3 Department of Endodontics, Dental School , Tabriz University of Medical Sciences , Tabriz , Iran
4 Drug Applied Research Center, Tabriz University of Medical Sciences, Tabriz, Iran; s.davaran2018@gmail.com (S.D.);
5 Stem cell research center, Tabriz University of medical sciences, Tabriz Iran; Lroshangar@yahoo.com (L.R.);
6 Stem Cell Research Center and Department of Oral Medicine, Tabriz University of Medical Sciences; aghazadeh.m@tbzmed.ac.ir (M.A.);
* Correspondence: sshahriar32@gmail.com (S.S.); aghazadeh.m@tbzmed.ac.ir (M.A.);

Scopus Author ID 21835058500
Received: 2.07.2020; Revised: 16.07.2020; Accepted: 16.07.2020; Published: 18.07.2020

Abstract: Bone has self-healing potential, but this characteristic is limited and requires external intervention. Bone formation is a dynamic process influenced by various growth factors. Angiogenesis is a fundamental phase and essential in the early stages of bone regeneration. Because of insufficient vascularization within osteoconductive or osteoinductive bone scaffolds, VEGF can be loaded into the scaffolds structure to induce blood vessels throughout engineered tissue. For this propose, PLA-g-P(HEM-co-NIPAAM) copolymers with HEMA:NIPAAm ratio of 1:1 and 1:5 are synthesized, and their biocompatibility, swelling, and vascular endothelial growth factor release properties are investigated. The hydrogels were biocompatible, and the cell attachment and growth were increased facing these hydrogels. The swelling performance of the synthesized hydrogels is increased by increasing the PHEMA ratio in the copolymer, which leads to high loading capacity. Different specifications for percent released over different time periods were achieved for the as-synthesized hydrogel, which will play a powerful role in bone regeneration in the near future.

Keywords: Thermosensitive Hydrogel; N-isopropylacrylamide (NIPAAm); 2-Hydroxyethyl - methacrylate (HEMA); Copolymer; Vascular endothelial growth factor (VEGF); Release.

1. Introduction

Oral cancer involves a wide range of malignant neoplasms that occur in the mouth. More than 90% of cases are squamous cell carcinoma (SCC). It originates more from epithelial tissue, salivary glands, and other types of tissue such as sarcoma and lymphoma. Metastasis is also involved in other parts of the body that are more likely to be lung, breast, prostate, and kidney. Most oral cancers occur in patients over the age of 40 and increase every ten years after the age of forty to sixty [1]. Dental removal and treatment for these patients are performed under high oxygen and inpatient conditions, with minimal tissue trauma. Current treatments for bone lesions, including the use of autogenous grafts, allografts, and bone powders, are

challenging in these patients [2,3]. In recent years, implantation of osteoblasts or mesenchymal stem cells that are exposed to osteogenic stimuli has had acceptable results in bone lesions [4].

It is clear that growth factors can promote the techniques of angiogenesis, osteogenesis, and bone repair. Vascular endothelial growth factor (VEGF) is one of the factors influencing angiogenesis [5]. Hydrogels due to their high tissue similarity and due to their water permeability and high capacity to hold water due to their biocompatibility, biodegradability, ease of manipulation of physical properties, drug protection against aggressive environmental factors and mechanical properties [6-8], therefore, ideal for cellular support and tissue regeneration, widely used as cellular matrix and scaffold for use in regenerative medicine [9, 10]. For this purpose, synthetic and natural hydrogels are used to regenerate various tissues, including cartilage, adipose, bone, vascular, etc. in general methods for stem cell engineering through the hydrogel network [11, 12]. Thus hydrogel-driven growth factor and delivery systems act as both a physical barrier to stabilize the cells implanted in the site and the defective region and provide a microenvironment for the formation of new tissue with a defined structure.

Some of the synthetic hydrogels used to repair bone and cartilage tissue are polyethylene glycol (PEG), polyethylene oxide (PEO), polylactic acid (PLA), polyglycolic acid (PGA), poly-lactic-co-glycolic acid. Acid (PLGA), polyethylene glycol diacrylate (PEGDA), polycaprolactone (PCL), polyvinyl alcohol (PVA), acrylic acid (AA), polypropylene fumarate (PPF), N-isopropylacrylamide (NIPAAM) and propylacrylic acid (PAA). One of the most important advantages of synthetic polymers is its ability to manipulate and control their desired properties [13-16]. Hydrogel systems that are chemically-crosslinked gels are desirable because they can be sensitive to both pH and temperature, for example, p(NIPAAm-co-alkyl(acrylic acid)), comb-type grafted p(NIPAAm-co-AA) and (p(NIPAAm-co-PAA)) gels have different swelling behavior for both pH and temperature changes [17-21]. In another study, thermosensitive gels containing NIPAAm, acrylic acid, and 2-hydroxyethyl methacryl lactate (HEMA-lactate) was investigated [22].

In the present study, biodegradable, biocompatible, and thermosensitive hydrogel scaffolds based on novel three-block PLA-g-P(HEM-co-NIPAAM) copolymers are synthesized, and the best hydrogel's vascular endothelial growth factor release property is investigated.

2. Materials and Methods

2.1. Materials.

The N-isopropylacrylamide (NIPAAm), 2-Hydroxyethylmethacrylate (HEMA), and stannous octoate (Sn (Oct)$_2$) were purchased from Sigma-Aldrich, USA. The dioxane and benzoyl peroxide were obtained from Merck Millipore, Germany. All materials used in this research were of analytical reagent grade and were used without further purification.

2.2. Synthesis of the hydrogels.

2.2.1. PLA-g-P(HEM-co-NIPAAM) copolymer.

To synthesize the macromonomer, a certain amount of HEMA monomer with lactide was melted at 130°C after deoxygenation with inert gas. After the monomers have melted, the Sn (Oct)$_2$ catalyst (0.05% by weight of the monomers) was added at 130°C. The mixture was stirred at this temperature under nitrogen gas for 5 hours. The polyester macromonomer

precipitates with the onset of HEM due to cooling. The resulting polymer is purified by dissolution and precipitation by purification.

Purified macromonomer was dissolved in dioxane at the presence of benzoyl peroxide catalyst with variable molecular percentages of N-isopropyl acrylamide (NIPAAm) to obtain a suitable copolymer (polyester-acrylate amphiphilic hybrid copolymers). The resulting copolymer was named as PPHN.

2.3. Characterization.

2.3.1. FT-IR.

Fourier transform infrared spectroscopy (Thermo Nicolet 5700 FT-IR spectrometer, Waltham, MA, USA), which equipped with germanium attenuated total reflection (ATR) accessory were used for the characterization of the chemical structure of the hydrogels.

2.3.2. Swelling tests.

The measurement of the temperature-dependent equilibrium swelling ratio was carried out gravimetrically on hydrogel samples. Each sample (50 mg) was weighed (Wd) and immersed inside 10 ml deionized water (pH 7.0) at 20 °C allowed to swell for at least 24h, then the temperature was increased step by step (stop 2 h at each temperature step) up to 40 °C. The excess water on the sample surface was removed by filter papers. Then the samples were weighted (Ww). The swelling ratio (Q) was calculated using the following equation [23]:

$$Q = (Ww – Wd) /Wd \quad (1)$$

2.4. Cell seeding and culture.

For cell culturing 10 mg of the hydrogel was placed in three siliconized 96-well cell culture plates (tissue culture-treated surface, Nunc). The scaffolds were sterilized by UV light overnight. Bone marrow stem cells in passage 4 were cultured in DMEM (Gibco) medium supplemented with 10% FBS (Cambrex) 100 $U.ml^{-1}$ penicillin (Gibco) 100 $\mu g.ml^{-1}$ streptomycin (Gibco) at 37ºC in a humid atmosphere with 5% CO_2 in a 75 ml culture flask. After reaching to 70-80%, confluence cells were detached by trypsinization (0.05% trypsin containing 1mM EDTA). Viable cells were counted by trypan blue assay and manual counting with a hemacytometer. Cells were seeded dropwise in the top of the scaffolds in the number of 5000 cells per scaffold. 200 µl of the culture medium was added to each well. The plate was kept the same condition as the incubator. Each plate was assessed after 1, 3, and 7 days. The medium was refreshed every 3 days. Cell proliferation was assessed using a dimethylthiazol diphenyltetrazolium bromide (MT) assay, which measured the mitochondrial dehydrogenase activity of vital cells by spectrophotometric. On the mentioned days, 50 µl of the medium was taken out, and 50 µl of MTT solution added. The cells were incubated for 4 hours at 37ºC. Addition of 50 µl of a mixture of dimethyl sulfoxide (DMSO) and Sorenson's buffer (8/1) reduced MTT by the mitochondrial dehydrogenase of normally metabolized cells to purple formazan. The plate was shaken for 15 minutes by a shaker. The upper solution was transferred to another 96 well plates, and the result was examined by spectrophotometry using a microplate ELISA reader (Multiskan MK3, Thermo Electron Corporation, USA) at 570 nm. The reference wavelength was 690 nm. Experiments were run in triplicate on each sample. Each sample had a control well containing the same count of cells and the same culture medium without scaffold.

For statistical significance, ANOVA and t-test were used to compare different groups. The P values < 0.05 were considered significant.

2.5. Loading and Release of VEGF.

Loading with VEGF was done by swelling 0.06 g of each dried hydrogels in the PBS buffer solution of 0.3 µg/mL of VEGF at 4°C for 3 days. The volume used was adjusted to load 0.1 µg VEGF per each mg of dried hydrogel (PPHN). The polymeric particles were then centrifuged and collected in order to study the VEGF release profile. For this propose, 500 µl of fresh PBS buffer was added to the as-prepared samples suspension. The microtubes were subsequently incubated at 37°C. At various time points, the samples were centrifuged at 12000 rpm for 10 min, 100 µl of the supernatants were collected, followed by the addition of 100 µl of the fresh PBS buffer to the polymeric suspensions and subsequent incubation. The cumulative percentage release of VEGF in the collected supernatant was determined using the VEGF Enzyme-linked Immunosorbent Assay (ELISA) Kit, according to the manufacturer's instructions.

3. Results and Discussion

3.1. Hydrogels synthesis and characterization.

The PPHN hydrogel was synthesized by free-radical polymerization using monomer NIPAAm, HEMA, and PLA at two different monomer ratios (Fig. 1). The resulting hydrogels were characterized in terms of their composition, swelling, cytocompatibility, and growth factor release properties.

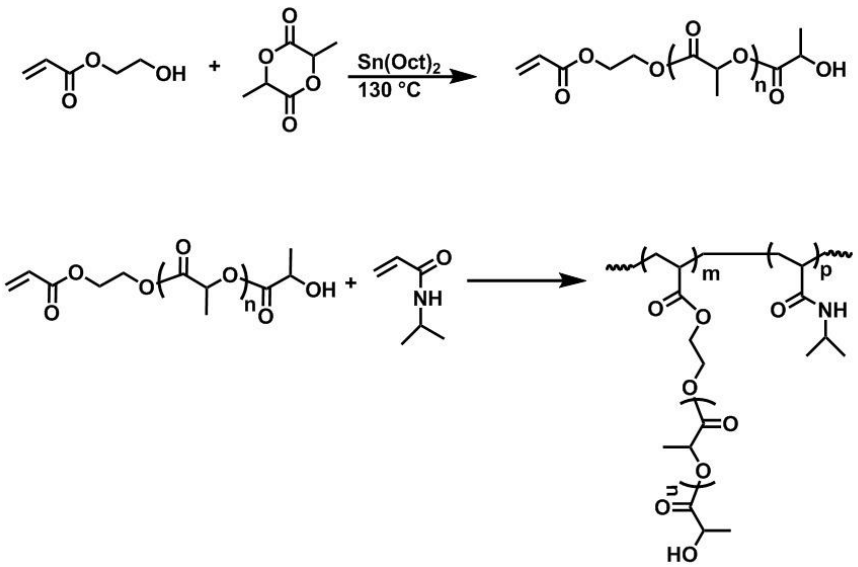

Figure 1. Schematic synthesis route of PPHN copolymer.

In Figure 2, the FT-IR spectrum of the as-synthesized PPHN copolymer was shown. Stretching vibrations of the ester carbonyl group showed at 1735 cm^{-1}. A broadband peak appeared between 3310 and 3434 cm^{-1} is due to N-H stretching group in PNIPAAm [24]. Peaks at 1646 cm^{-1} and 1383 cm^{-1} corresponding to the amide group and the C-H vibrations of -$CH(CH_3)_2$ in the PNIPAAm, respectively.

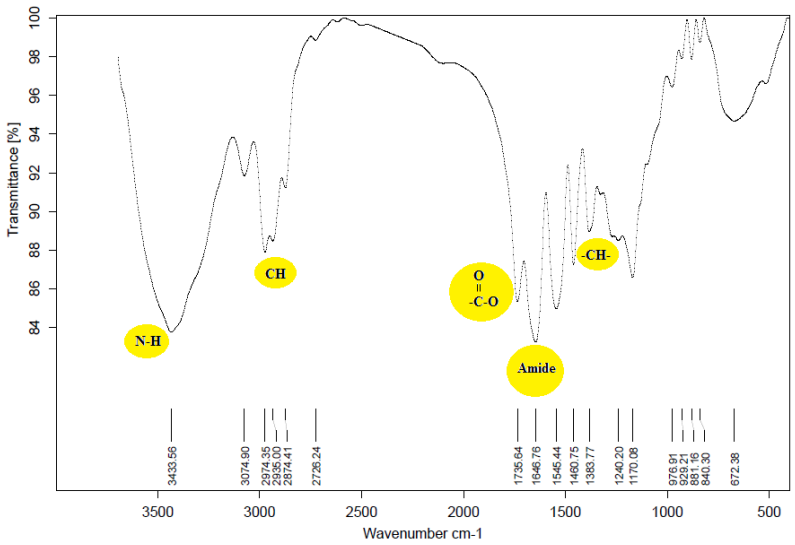

Figure 2. FT-IR spectra of PPHN5 copolymers.

The effect of polymer composition on the swelling ratio of gels in the water at a temperature in the range of 20 ºC to 40 ºC is given in Figures 3. Three different polymers were used PNIPAAM, PNIPAAM-co-PHEMA (molar ratio of 5:1), and PNIPAAM-co-PHEMA (molar ratio of 1:1). It can be seen from these Figures that by increasing the PHEMA ratio in the copolymer, the swelling ratio was increased. The lowest swelling ratio was observed in PNIPAAM, and the swelling ratio was decreased gradually and reached to zero at PNIPAAM LCST(35 ºC). Also, gels exhibit significant continuous changes in swelling ratio values in which the swelling ratio decreased with temperature increase. Therefore we observed a consequence of volume collapse upon warming. These figures show that the swelling ratio of gels is dependent not only on the temperature but also on the polymer composition.

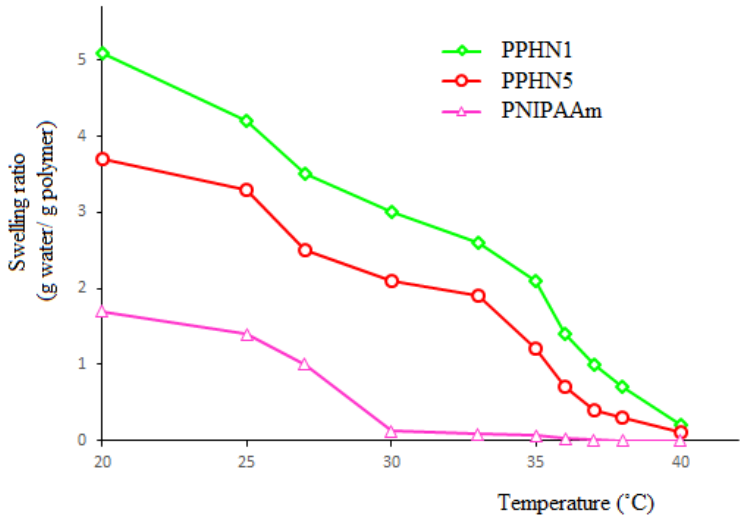

Figure 3. Swelling ratio of gels in the water at 20 ºC to 40 ºC.

3.2. Cell seeding and culture.

Hydrogels are attracting more attention in tissue engineering and regenerative medicine. Their surface properties and mechanical characteristics mimic the natural extracellular matrix. PNIPAM hydrogels are discussed in a wide range of studies due to their soft texture and thermal sensitivity. Biocompatibility is a basic and essential assay for any

material to be applied in the clinic. Routinely the viability of different cells is compared with and without facing the material. The alteration of mitochondrial activity is the standard criteria in this regard.

In our study, we evaluated the proliferation of bone marrow stem cells on 3 types of scaffolds containing NIPAAm and HEMA groups. The control group contained bone marrow cells and culture medium (figure 4). These cells were not exposed to scaffolds. In all cases, an increase in mitochondrial activity was observed. This proliferation was higher in the PPHN5 group. No cytotoxic effect was observed in case groups. All of the scaffolds were safe and induced cell proliferation in 1, 3, and 5 days. In comparison with the cell growth in PPHN1, PPHN5, and PNIPAAm scaffolds, there is a significant difference between PPHN5 and other groups. This stimulation is obvious in all of the evaluated times. There is a decrease in the number of vital cells in the PNIPAAm group on days 1 and 3. However, it was followed by an increase in day 5. Due to statistical analysis, this effect was evaluated as mild cytotoxicity.

The cytotoxic effect of scaffolds containing PNIPAAm is related to the NIPAAm monomer [25]. The cytotoxic effect of this material is assessed on adipose, human embryonic kidney, and lung carcinoma epithelial cells [25]. There are few studies about its biocompatibility on mesenchymal stem cells. The results of this study were consistent with Rivero *et al*. study, which evaluated the cytotoxic effect of PNIPAAm hydrogel on bovine fetal fibroblasts (BFFs). They reported the safe effect of this material [26]. The same results were reported by Tebong Mbah *et al.* [27]. There was no genotoxic response of nanoparticles of PNIPAM in human keratinocyte [28] and human bronchial epithelial [29].

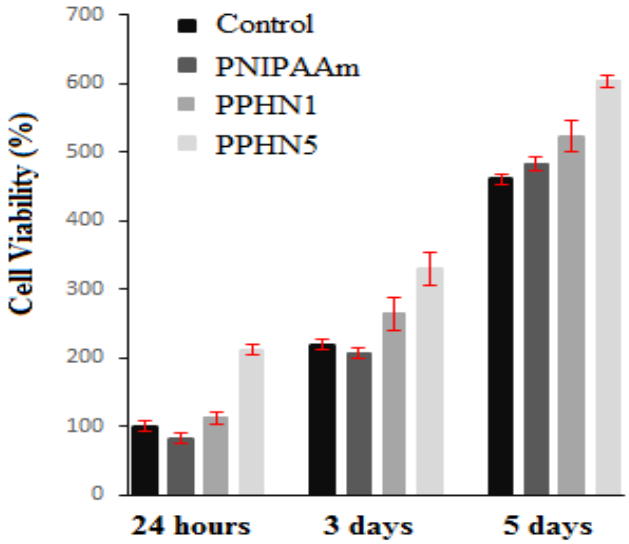

Figure 4. MTT assay of hBMSCs viability after treatment with gels. The standard deviations (±SD) were obtained on a fourfold analysis.

In our study, we observed mild cytotoxicity of PNIPAAm in the first and third days. The noticeable point is that this effect was completely eliminated in the PPHN1 and PPHN5 group due to a combination of NIPAAm with HEMA. This data showed that application of HEMA not only eliminates the cytotoxic effect of NIPAAm, but also improved the cell proliferation at the same time. Due to the results of this study, our designed hydrogel was biocompatible with bone marrow stem cells. The cell attachment and growth was increased facing to this hydrogel. This hydrogel could be purposed as a 2D and 3D scaffold for a potential application in tissue engineering of bone.

3.3. Release profile of VEGF.

VEGF is an important growth factor in angiogenesis. Bone is a vascular organ, and angiogenesis plays an important role in bone formation and bone remodeling [30]—. Radiotherapies due to oral cancer treatments effects on bone vasculogenesis and limits bone regeneration.

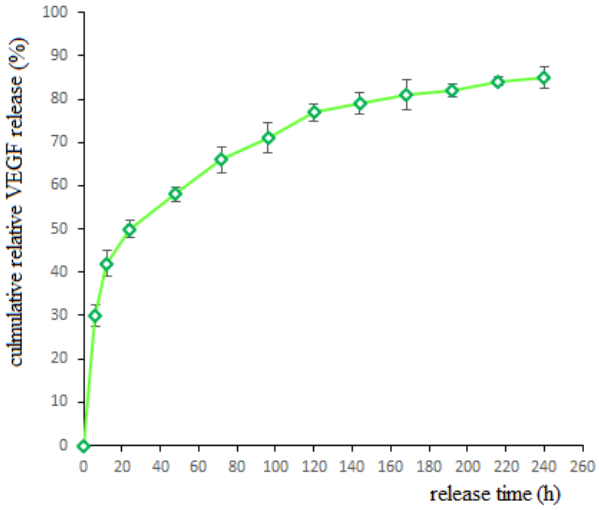

Figure 5. VEGF release profile from PPHN5 hydrogel.

Bone loss and bone necrosis, followed by radiotherapy, affect the oral and systemic health of patients with oral cancers. Bone allografts are applied as gold standards for bone regeneration, but success is highly related to new vascularization and blood supply [31]. Local application of VEGF in the defected area using sustained releasing biomaterials can play a crucial role. In our study, we introduced an implantable hydrogel with sustained release of VEGF. Due to the continuous and gradual release of VEGF, this biomaterial could be applied for the ossification of craniofacial and other bone defects. It could be applied locally alone or along with dental and bone implants to reduce healing time and increase the quantity and quality of new bone. In the process of normal bone healing, the expression of VEGF is at a maximum level in the early days [32], so a similar release profile would be beneficial. As shown in figure 5, the as-synthesized PPHN5 hydrogel mimics the natural expression with an initial VEGF burst release in the first 20 hours, and then followed with a fast release for 120 hours and almost linear sustained release for the rest time. This biomaterial could provide access to the VEGF growth factor in the required dose for bone formation.

4. Conclusions

PLA-g-P(HEM-co-NIPAAM) copolymer was successfully synthesized by a free radical method that had the capability to deliver VEGF. Based on the MTT assay, PNIPAM, PPHN1, and PPHN5 after 5 days had no statistically significant cytotoxicity on hBMSCs.

Development of biocompatible, degradable hydrogels with sustained released growth factors will undoubtedly become a strong and essential tool for surgeons and clinicians in bone defect treatments. Angiogenesis is a basic necessity in bone regeneration. Hydrogels mimicking the natural profile of VEGF release in the bone healing process will play a powerful role in bone regeneration in the near future.

Funding

This study was financially supported by the Tabriz University of Medical Sciences (Grant No. 59337).

Acknowledgments

The authors would like to thank the Dental and Periodontal Research Center and Tabriz University of Medical Sciences for supporting this project.

Conflicts of Interest

The authors declare no conflict of interest.

References

1. Falzone, L.; Lupo, G.; La Rosa, G.R.M.; Crimi, S.; Anfuso, C.D.; Salemi, R.; Rapisarda, E.; Libra, M.; Candido, S. Identification of Novel MicroRNAs and Their Diagnostic and Prognostic Significance in Oral Cancer. *Cancers* **2019**, *11*, https://doi.org/10.3390/cancers11050610.
2. Ribeiro, G.H.; Chrun, E.S.; Dutra, K.L.; Daniel, F.I.; Grando, L.J. Osteonecrosis of the jaws: a review and update in etiology and treatment. *Braz J Otorhinolaryngol* **2018,** *84*, 102-108, https://doi.org/10.1016/j.bjorl.2017.05.008.
3. Chambrone, L.; Mandia, Jr. J.; Shibli, J.A.; Romito, G.A.; Abrahao, M. Dental implants installed in irradiated jaws: a systematic review. *J Dent Res* **2013**, *92*, 119S-130S, https://doi.org/10.1177/0022034513504947.
4. Safarova, Y.; Umbayev, B.; Hortelano, G.; Askarova, S. Mesenchymal stem cells modifications for enhanced bone targeting and bone regeneration. *Regen. Med.* **2020,** 15, 1579–1594, https://doi.org/10.2217/rme-2019-0081.
5. Vining, K.H.; Mooney, D.J. Mechanical forces direct stem cell behaviour in development and regeneration. *Nat Rev Mol Cell Biol* **2017**, *18*, 728-742, https://doi.org/10.1038/nrm.2017.108.
6. Brianezi, S.F.; Castro, K.C.; Piazza, R.D.; Melo, M.D.; Pereira, R.M.; Marques, R.F.; Campos, M.G. Preparation and characterization of chitosan/mPEG-PCL blended membranes for wound dressing and controlled gentamicin release. *Mater Res* **2018**, *21*, https://doi.org/10.1590/1980-5373-mr-2017-0951.
7. Chaudhuri, S.; Wu, C.M. Switchable wettability of poly (NIPAAm-co-HEMA-co-NMA) coated PET fabric for moisture management. *Polymers* **2020**, *12*, 100, https://doi.org/10.3390/polym12010100.
8. Spicer, C.D. Hydrogel scaffolds for tissue engineering: the importance of polymer choice. *Polym Chem* **2020**, *11*, 184-219, https://doi.org/10.1039/C9PY01021A.
9. Mantha, S.; Pillai, S.; Khayambashi, P.; Upadhyay, A.; Zhang, Y.; Tao, O.; Pham, H.M.; Tran. S.D. Smart hydrogels in tissue engineering and regenerative medicine. *Materials* **2019**, 12, 3323, https://doi.org/10.3390/ma12203323.
10. Wu, S.W.; Liu, X.; Miller II, A.L.; Cheng, Y.S.; Yeh, M.L.; Lu, L. Strengthening injectable thermo-sensitive NIPAAm-g-chitosan hydrogels using chemical cross-linking of disulfide bonds as scaffolds for tissue engineering. *Carbohydr polym* **2018**, *192*, 308-316, https://doi.org/10.1016/j.carbpol.2018.03.047.
11. Kumar Meena, L.; Rather, H.; Kedaria, D.; Vasita, R. Polymeric microgels for bone tissue engineering applications–a review. *Int J Polym Mater Po* **2020**, *69*, 381-397, https://doi.org/10.1080/00914037.2019.1570512.
12. Vasile, C.; Pamfil, D.; Stoleru, E.; Baican, M. New Developments in medical applications of hybrid hydrogels containing natural polymers. *Molecules* **2020**, *25*, https://doi.org/10.3390/molecules25071539.
13. Wang, C.; Lu, W.W.; Wang, M. Multifunctional fibrous scaffolds for bone regeneration with enhanced vascularization. *J Mater Chem B* **2020**, *8*, 636-647, https://doi.org/10.1039/c9tb01520e.
14. Wang, S.; Yang, Y.; Koons, G.L.; Mikos, A.G.; Qiu, Z.; Song, T.; Cui, F.; Wang, X. Tuning pore features of mineralized collagen/PCL scaffolds for cranial bone regeneration in a rat model. *Mater Sci Eng C* **2020**, *106*, https://doi.org/10.1016/j.msec.2019.110186.
15. Pang, L.; Shen, Y.; Hu, H.; Zeng, X.; Huang, W.; Gao, H.; Wang, H.; Wang, D. Chemically and physically cross-linked polyvinyl alcohol-borosilicate gel hybrid scaffolds for bone regeneration. *Materials Science and Engineering: C* **2019,** *105*.
16. García-García, P.; Reyes, R.; Segredo-Morales, E.; Pérez-Herrero, E.; Delgado, A.; Évora, C. PLGA-BMP-2 and PLA-17β-Estradiol microspheres reinforcing a composite hydrogel for bone regeneration in osteoporosis. *Pharmaceutics* **2019**, *11*, https://doi.org/10.3390/pharmaceutics11120648.
17. Brazel, C.S.; Peppas, N.A. Synthesis and characterization of thermo-and chemomechanically responsive poly (N-isopropylacrylamide-co-methacrylic acid) hydrogels. *Macromolecules* **1995**, *28*, 8016-8020, https://doi.org/10.1021/ma00128a007.

18. Frazar, E.M.; Shah, R.A.; Dziubla, T.D.; Hilt, J.Z. Multifunctional temperature-responsive polymers as advanced biomaterials and beyond. *J Appl Polym Sci* **2020**, *137*, https://doi.org/10.1002/app.48770.
19. Dadfar, S.M.; Pourmahdian, S.; Tehranchi, M.M.; Dadfar, S.M. Novel dual-responsive semi-interpenetrating polymer network hydrogels for controlled release of anticancer drugs. *J Biomed Mater Res A* **2019**, *107*, 2327-2339, https://doi.org/10.1002/jbm.a.36741.
20. Yin, X.; Hoffman, A.S.; Stayton, P.S. Poly (N-isopropylacrylamide-co-propylacrylic acid) copolymers that respond sharply to temperature and pH. *Biomacromolecules* **2006**, *7*, 1381-1385, https://doi.org/10.1021/bm0507812.
21. Garbern, J.C.; Hoffman, A.S.; Stayton, P.S. Injectable pH-and temperature-responsive poly (N-isopropylacrylamide-co-propylacrylic acid) copolymers for delivery of angiogenic growth factors. *Biomacromolecules* **2010**, *11*, 1833-1839, https://doi.org/10.1021/bm100318z.
22. Lee, B.H.; Vernon, B. In situ-gelling, erodible N-isopropylacrylamide copolymers. *Macromol Biosci* **2005**, *5*, 629-635, https://doi.org/10.1002/mabi.200500029.
23. Zhang, X.Z.; Lewis, P.J.; Chu, C.C. Fabrication and characterization of a smart drug delivery system: microsphere in hydrogel. *Biomaterials* **2005**, *26*, 3299-3309, https://doi.org/10.1016/j.biomaterials.2004.08.024.
24. Saghebasl, S.; Davaran, S.; Rahbarghazi, R.; Montaseri, A.; Salehi, R.; Ramazani, A. Synthesis and in vitro evaluation of thermosensitive hydrogel scaffolds based on (PNIPAAm-PCL-PEG-PCL-PNIPAAm)/Gelatin and (PCL-PEG-PCL)/Gelatin for use in cartilage tissue engineering. *J Biomater Sci Polym Ed* **2018**, *29*, 1185-1206, https://doi.org/10.1080/09205063.2018.1447627.
25. Capella, V.; Rivero, R.E.; Liaudat, A.C.; Ibarra, L.E.; Roma, D.A.; Alustiza, F.; Mañas, F.; Barbero, C.A.; Bosch, P.; Rivarola, C.R.; Rodriguez, N. Cytotoxicity and bioadhesive properties of poly-N-isopropylacrylamide hydrogel. *Heliyon* **2019**, *5*, https://doi.org/10.1016/j.heliyon.2019.e01474.
26. Rivero, R.; Alustiza, F.; Capella, V.; Liaudat, C.; Rodriguez, N.; Bosch, P.; Barbero, C.; Rivarola, C. Physicochemical properties of ionic and nonionic biocompatible hydrogels in water and cell culture conditions: relation with type of morphologies of bovine fetal fibroblasts in contact with the surfaces. *Colloids Surf B Biointerfaces* **2019**, *158*, 488-497, https://doi.org/10.1016/j.colsurfb.2017.07.032.
27. Tebong Mbah, V.; Pertici, V.; Lacroix, C.; Verrier, B.; Stipa, P.; Gigmes, D.; Trimaille, T. A sacrificial PLA block mediated route to injectable and degradable PNIPAAm-based hydrogels. *Polymers* **2020**, *12*, https://doi.org/10.3390/polym12040925.
28. Nguyen, P.A.H.; Stapleton, L.; Ledesma-Mendoza, A.; Cuylear, D.L.; Cooperstein, M.A.; Canavan, H.E. Exploring the anomalous cytotoxicity of commercially-available poly(*N*-isopropyl acrylamide) substrates. *Biointerphases* **2018**, *13*, https://doi.org/10.1116/1.5045142.
29. Rivero, R.E.; Capella, V.; Liaudat, A.; Bosch, P.; Barbero, C.; Rodríguez, N.; Rivarola. C. Mechanical and physicochemical behavior of a 3D hydrogel scaffold during cell growth and proliferation. *RSC Adv* **2020**, *10*, https://doi.org/10.1039/C9RA08162C.
30. Farré-Guasch, E.; Bravenboer, N.; Helder, M.N.; Schulten, E.A.J.M.; Ten Bruggenkate, C.M.; Klein-Nulend, J. Blood vessel formation and bone regeneration potential of the stromal vascular fraction seeded on a calcium phosphate scaffold in the human maxillary sinus floor elevation model. *Materials (Basel)* **2018**, *11*, https://doi.org/10.3390/ma11010161.
31. Fernandez de Grado, G.; Keller, L.; Idoux-Gillet, Y.; Wagner, Q.; Musset, A.M.; Benkirane-Jessel, N.; Bornert, F.; Offner, D. Bone substitutes: a review of their characteristics, clinical use, and perspectives for large bone defects management. *J Tissue Eng* **2018**, *9*, https://doi.org/10.1177/2041731418776819.
32. Kempen, D.H.R.; Lu, L.; Heijink, A.; Hefferan, T.E.; Creemers, L.B.; Maran, A.; Yaszemski, M.J.; Dhert, W.J.A. Effect of local sequential VEGF and BMP-2 delivery on ectopic and orthotopic bone regeneration. *Biomaterials* **2009**, *30*, 2816-2825, https://doi.org/10.1016/j.biomaterials.2009.01.031.